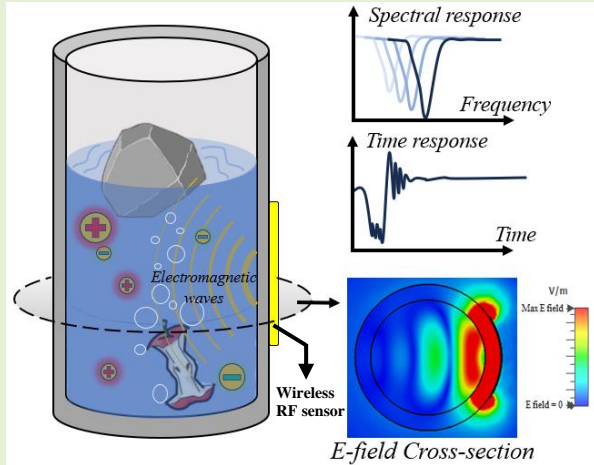


Time-Transient Wireless RF Sensor with Differentiative Detecting Capability for Target Ionic Solution of Water and Dielectric Objects Introduced into Water

Sobhan Gholami, Emre Unal, and Hilmi Volkan Demir, *Fellow Member, IEEE*

Abstract— A novel wireless microstrip-based RF sensor designed for detecting changes in ionic content of water and the addition of solid contaminant objects is proposed and demonstrated. The sensor can be installed on the exterior wall of dielectric containers and customized according to the material of the container to enable wireless sensing. Its operation within the lower microwave frequency range (670-730 MHz) serves to minimize signal attenuation in water and streamlines circuitry design. The most significant feature of this sensor is its unique design, rendering it impervious to its surrounding environment. This not only shields it from environmental noise but also maximizes its sensitivity by efficiently utilizing incoming power for sensing purposes. The sensor exhibits remarkable sensitivity, capable of detecting solute concentrations as low as 3.125×10^{-3} M in water. It can also detect the insertion of foreign solid objects into the container from the exterior wirelessly and distinguish them from liquids being added. As a proof-of-concept demonstration, the sensor in this study was optimized for a porcelain wall of 10-12 mm thickness. The sensor's small size and the materials used for its fabrication make it adaptable to a wide range of applications in industries such as food, pharmaceuticals, and bathroom fixtures. The aforementioned properties position the sensor as an ideal choice for various smart bathroom applications, where accurate and reliable water use monitoring is essential for efficient water conservation.

Index Terms—Microstrip patch antenna, microwave propagation, microwave sensors, chemical and biological sensor, signal analysis, water conservation, water monitoring, green cleaning.



I. Introduction

In recent years, the pressing issue of global warming and its effect on water resources [1], [2], [3], has attracted much attention in using technology for water conservation. There have been efforts in the reduction of water use, especially in bathrooms, as a significant source of water consumption at homes by imposing regulations [4]. In addition, new toilet designs have been introduced that require less water for flushing [5], [6]. Sensors have also been employed to promote water conserving practices in bathroom facilities. Examples of such sensors are IR proximity sensors for automatic urinal flushing in public bathrooms, as well as load detectors installed under toilet lids for automatic flushing [7], [8].

This paper was submitted for review on 25.01.2024. This project is supported by TUBITAK's Industry Innovation Network Mechanism (SAYEM) Program under grant no. 121D010 (Akıllı Ev Platformu).

S. Gholami is a graduate student with the department of Electrical and Electronics Engineering, Bilkent University, TR-06800, Ankara, Turkey (e-mail: gholami@ee.bilkent.edu.tr).

E. Unal is with the Institute of Materials Science and Nanotechnology, Bilkent University, TR-06800 Ankara, Turkey (e-mail: unale@bilkent.edu.tr).

While IR sensors activate the flushing mechanism based on the reflection of electromagnetic wave (EMW) of a specific wavelength from the presence of an object or person in front of the sensor, in load sensors, mechanical energy is converted into electrical signals to show the presence of a person sitting on the lid and obviate the need to mechanically press the flush button or press it multiple times unnecessarily after standing up. Yet non operates based on the actual presence of excreta in the toilet.

To address the sanitation concerns, it is advisable to utilize electromagnetic waves for sensing in bathrooms. EMW's do not require physical contact with human excreta and thus minimize unwanted contamination. A considerable number of

H. V. Demir is with the Department of Electrical and Electronics Engineering and the Department of Physics, Institute of Materials Science and Nanotechnology (UNAM), Bilkent University, TR-06800 Ankara, Turkey, and also with the School of Electrical and Electronic Engineering and the School of Physical and Mathematical Sciences, Nanyang Technological University, Singapore 639798 (e-mail: volkan@bilkent.edu.tr).

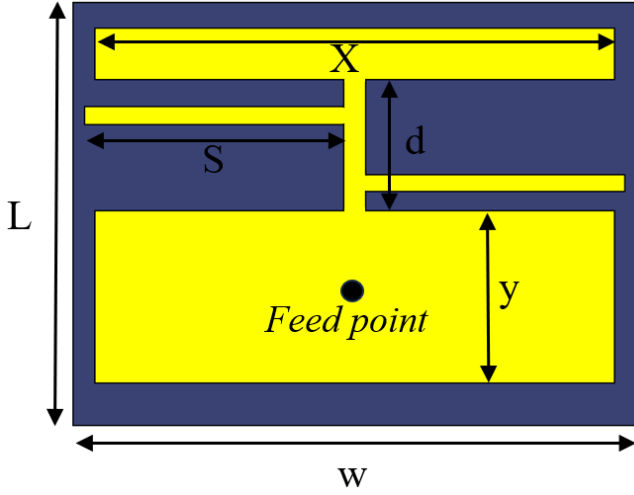


Fig. 2. Proposed sensor's structure. $W=65$ mm, $L=50$ mm, $d=15.2$ mm, $S=30$ mm, $x=60$ mm, $y=23$ mm.

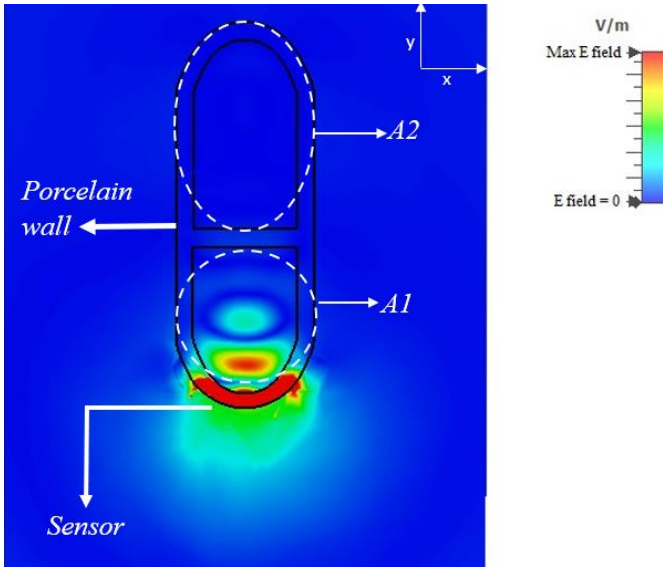


Fig. 3. Z-cut representation of propagation of EMW through porcelain into water. A1 is the front side of the S pipe underneath the toilet bowl, where the excreta are first inserted. A2 is in the outgoing part of the S pipe.

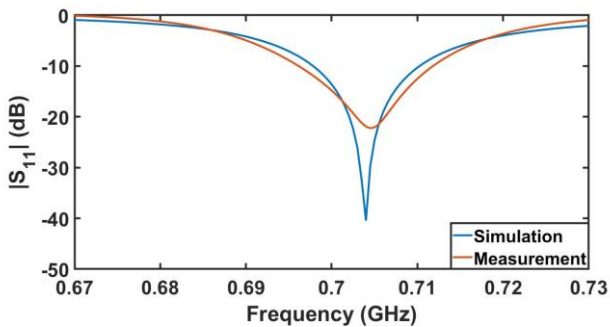


Fig. 4. Experimentally measured reflection coefficient compared to numerical solution of the fabricated sensor.

where Z_0 represents the intrinsic impedance of the line, Z_L the terminating load and l , the length of the line. Setting $Z_L = \infty$ for an open-ended transmission line makes:

$$Z_{in} = -jZ_0 \cot \beta l \quad (2)$$

According to (2), the open-ended transmission line can provide almost any reactance by tuning the length and the intrinsic impedance of the line. The intrinsic impedance of the line is determined using [33]:

$$Z_0 = \frac{120\pi}{\sqrt{\epsilon_{eff}} \left[\frac{w}{h} + 1.393 + 0.667 \ln \left(\frac{w}{h} + 1.44 \right) \right]} \quad (3)$$

$$\epsilon_{eff} = \frac{\epsilon_r + 1}{2} + \frac{\epsilon_r - 1}{2} \left[1 + 12 \frac{h}{w} \right]^{-1/2} \quad (4)$$

In (3) and (4), w is the width of the stub; h is the height of the underlying dielectric substrate and ϵ_r is the relative dielectric constant of the substrate.

To implement the stub, a 50-ohm microstrip transmission line was drawn between the patch and tuning patch. Two open-ended stubs were introduced on both sides of the line to provide capacitance. The location of the stubs from the tuning patch, their length and length of the transmission line was tuned using Computer Simulation Technology Microwave Studio to achieve the lowest resonant frequency possible. The sensor was designed on Rogers corporations RT5880 double sided copper with dielectric thickness of 0.79 and copper thickness of 0.018 mm shown in Fig. 2.

As the sensor's primary objective is to transmit EMW through porcelain into water, the tuning and optimization process was conducted within a porcelain medium immersed in water. This approach closely emulates the sensor's real operational conditions. By adopting this optimization method, reflections from the sensor/porcelain interface were minimized, allowing a higher proportion of the source power to penetrate the medium and facilitate sensing. Fig. 3 visually represents the electric field radiated by the sensor into the medium, demonstrating the sensor's ability to remain isolated from its surrounding environment—a key accomplishment sought in our design.

The design was physically realized on a double-sided copper laminate of Rogers corporations RT5880 (with $\epsilon_r=2.2$ and $\tan \delta=0.009$). Experimental testing was carried out on a porcelain container with a thickness between 10 to 12 mm. A comparison between numerical simulations and measurement results are presented in Fig. 4 where acceptable agreement between the numerical solutions and measurements is achieved.

III. RESULTS AND DISCUSSION

The proposed sensor is capable of detecting the change in the concentration of water and sense the insertion of dielectric objects in the toilet. To evaluate the capability of the designed sensor for practical application, a special structure is designed to emulate the actual situation in a bathroom. The sensor is hot

glued to the front section of the S pipe on the bottom of the porcelain toilet setup and it communicates with an Agilent technologies E5061B ENA through a SMA cable shown in the inset of Fig. 5. Careful attention was given to thoroughly remove all air gaps between the sensor and the porcelain to prevent multiple reflections between the two surfaces.

To test the sensor and determine its sensing range in response to changes in the ion content of water, we prepared samples of NaCl solutions with different concentrations in the range of 3.125×10^{-3} to 5.000×10^{-1} M (mol/L) using 99.9% pure NaCl. Additionally, we prepared an artificial urine solution following the formulation provided in [34] and maintained it at 37 °C. This allowed us to determine which concentrations of NaCl solutions at room temperature yield an equivalent electrical response when added to water instead of artificial urine.

In order to emulate the addition of feces to the medium, samples were prepared using the formulation in [35], which weigh around 45-50 gr each.

A. Detecting the change in ionic concentration of water

The electrical response of a material to the incident electromagnetic wave is determined by its dielectric constant. The dielectric constant of pure water is well described by Debye model as a function of the frequency [36]:

$$\epsilon_w(f) = \epsilon_w(\infty) + \frac{\epsilon_w(0) - \epsilon_w(\infty)}{1 + i2\pi f\tau_w} \quad (5)$$

where $\epsilon_w(\infty)$ is the dielectric constant of water at very high frequency, $\epsilon_w(0)$ is the dielectric constant of water at DC and τ_w is the relaxation time of pure water. Since (5) spans a broad frequency spectrum, it is reasonable to assume that the dielectric constant of water remains constant within the operational frequency range of this work (670-730MHz).

When ions are dissolved in pure water, the DC dielectric constant of water and relaxation time are influenced by the presence of ions, resulting in modifications to the relation described in (5) [37]:

$$\epsilon_s(f) = \epsilon_w(\infty) + \frac{\epsilon_s(0) - \epsilon_w(\infty)}{1 + i2\pi f\tau_s} - i \frac{\delta}{2\pi f\epsilon_0} \quad (6)$$

Here ϵ_0 is the dielectric permittivity of free space, ϵ_s is the static dielectric constant, τ_s is the relaxation time, and δ is the conductivity of the resultant solution, which are functions of the concentration of the dissolved ions. Detailed relationships governing these properties can be found in [37], [38], [39]. The introduction of an ionic solution with a concentration higher than that of water alters the ion content of the water, leading to changes in ϵ_s . These changes manifest as variations in the electrical response of the solution which in the case of this study, is the changes in the frequency of minimum reflection coefficient (S11).

To examine changes in the sensor's steady-state reflection coefficient, the toilet was filled with water containing various concentrations of NaCl. We analyzed the resulting resonance frequency shift ($f - f_0$) concerning the baseline case when the medium consisted of only water (f_0). These comparisons are

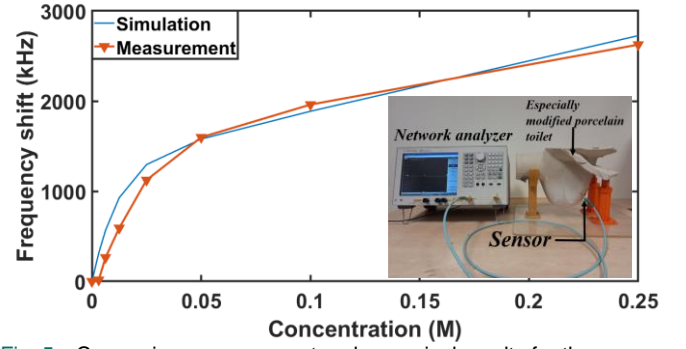


Fig. 5. Comparing measurement and numerical results for the frequency shift corresponding to various concentrations of NaCl in the measurement setup in the inset.

visually represented in Fig 5. It is clearly seen that the increase in the ion content of the medium, leads to a consistent shift in the resonance frequency.

In the next step to observe the transient sensor response to the addition of ions, 200 ml volumes of solutions with concentrations of 3.125×10^{-2} , 6.25×10^{-2} , 1.25×10^{-1} , 2.5×10^{-1} , 5×10^{-1} M and artificial urine were slowly injected into the test toilet setup, simulating the introduction of urine into the medium. Fig 6. shows the shifts in the frequency vs volume of added solution for different solution concentrations. Horizontal dashed lines show the concentration of the medium. Step by step, as more solution was added to the medium while the volume was constant, the shift in the frequency monotonously increased.

Since we expect an exponential response from the addition of ions into the system, we fitted the data points using:

$$\Delta f = a(1 - e^{-bv}) \quad (7)$$

Here a represents the maximum frequency shift expected to occur in steady state and b determines the rate at which the steady state is reached. v is the volume of solution in mL added.

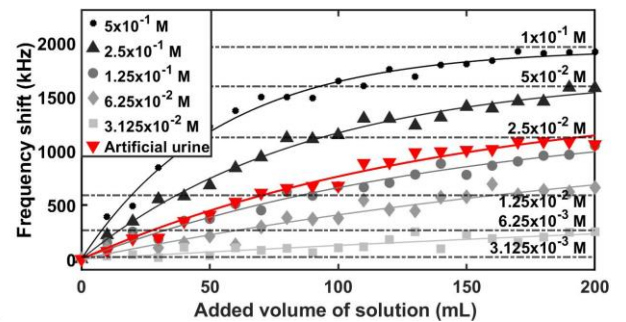


Fig. 6. Measurement results of changes in resonance frequency (frequency shift) with respect to the volume of added NaCl solution with different concentrations. Horizontal dashed lines show the frequency shift corresponding to concentration of the mixture inside the toilet.

B. Simultaneously detecting the addition of solid objects into water in contrast to the ionic solution

The introduction of solid objects into a medium, when compared to the addition of solutions, often leads to significant and erratic shifts in resonance frequencies. Therefore, the transient response becomes a crucial aspect to consider. In the context of our study, when a solid object is introduced into the water, it generates ripples on the water's surface, with the amplitude of these ripples directly reflecting the energy associated with the inserted object. Consequently, analyzing the amplitude of these ripples serves as a valuable means of determining the presence of feces within the toilet. The sensor, loaded with water in design, captures and registers the ripples produced, which, in turn, induce direct changes in its resonance frequency. As a consequence, these ripples manifest as distinctive features on the frequency shift curve over time. Analyzing the frequency content of this time-dependent frequency shift curve offers distinctive features to differentiate feces from ionic solution.

To isolate the ripples from the frequency shift curve, we performed an instantaneous differential operation on the frequency shift data. This operation effectively eliminates any influence from the presence of solid objects within the sensor's electromagnetic field. Following this step, we employ Fourier transformation to obtain the frequency components within the derivative of the frequency shift curve.

For the Fourier analysis, it is important to consider the sampling time of the signal. In our study, we set a consistent sampling time of 110 ms between each data point. Fig. 7 illustrates the three critical stages of detecting, analyzing and comparing the ripples in the solid object insertion case together with the liquid injection case. For the most comprehensive examination, we conducted tests involving liquid injection from a height of 80 cm above the water level at a rate of 17 mL/s [40]. In Fig. 7(a), we present the frequency shift curve resulting from the introduction of three 50-gram pieces of artificial feces compared with injection of 220 mL of 1.25×10^{-1} M solution of NaCl. Fig. 7(b) showcases the derivative of the frequency shift curve ($\frac{d(f-f_0)}{dt}$) for both these cases, and in Fig. 7(c), we present the Fourier transform of the frequency shift curves. Two prominent frequency peaks within the range of 1.6 to 3.0 Hz are clearly observed in our analysis of solid insertion case. These peaks correspond to the dominant period of water ripples due to the depth of water in the toilet [41]. Significantly, these peaks consistently show up with noticeable magnitudes whenever a solid object is introduced into the water.

As it is expected (Fig. 7(c)) ripples generated by the injection of liquids into the toilet exhibit substantially smaller magnitudes within the modulation frequency range of 1.6 to 3.0 Hz compared to instances involving solid object insertion. Naturally, feces displace greater amounts of water leading to higher amplitudes of waves formed on the surface. This allows to differentiate between the insertion of feces and urine into the toilet via analyzing the spectrum of the filtered data shown in Fig. 7(b). We achieve this by applying a bandpass filter and conducting spectral analysis on the frequency content of the derivative curve, ($\frac{d(f-f_0)}{dt}$), at regular time intervals. Following

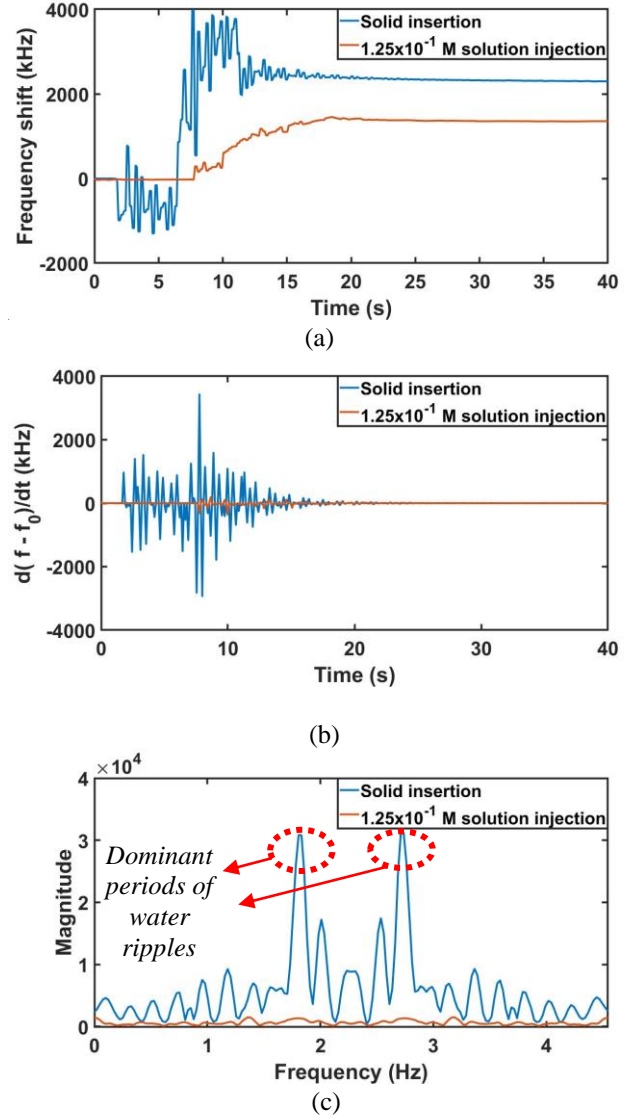


Fig. 7. Measurement and analysis of injection of 1.25×10^{-1} M solution with insertion of solids into the medium: (a) frequency shift curves corresponding to both cases, (b) derivative of the frequency shift curves in both cases, and (c) frequency content of the derivative of frequency shift curve.

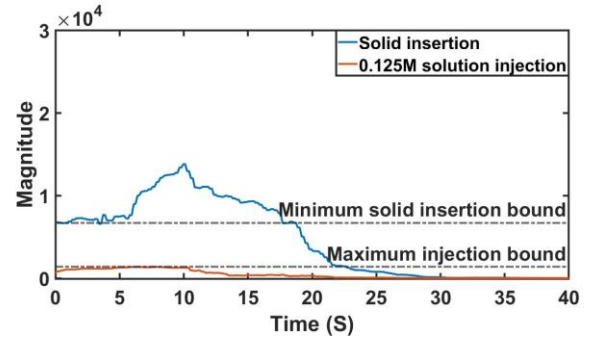


Fig. 8. Comparing minimum and maximum detected sensing signal magnitude of solid insertion and 1.25×10^{-1} M NaCl solution injection.

this approach also enables us to track the magnitude of the peaks within the 1.6 – 3.0 Hz range over time.

In Fig. 8, we selected the scenario with the lowest magnitude out of 9 tests for solid insertion and compared it to the injection case where the highest magnitude was reached. This comparison reveals a significant difference between these two extreme scenarios, underscoring the reliability of this analysis method in distinguishing between the incoming of feces and urine in the toilet.

In this case study, the sensing algorithm is structured as follows: initially, the system conducts a comprehensive scan to identify the presence of solid insertions, promptly executing a washing procedure upon detection. The performed washing also removes any potential ionic solutions. In instances where no solid insertions are detected, the system shifts its focus to analyzing the resonance frequency's shift, specifically corresponding to the introduction of electrolytes. This analytical approach enables the system to discern the concentration of the added solution, empowering it with the capability to execute programmable actions commensurate with the concentration level.

IV. CONCLUSION

A novel wireless sensor design capable of distinctly detecting changes in the ionic content of water and the insertion of solid objects in dielectric container is introduced. The sensor detects changes as low as 3.125×10^{-3} M in the ionic content of water and distinguishes between the responses related to the alteration in the concentration of water and insertion of solid objects. Measurements were carried out and results agreed with the expectations from numerical solutions. The application of the sensor in this particular case study can greatly improve the water conservation in public bathrooms and shopping centers. Moreover, its wireless functionality and ability to sense through non-metallic walls position it as a versatile tool for applications in pharmaceutical, chemical, and food industries. The strategic use of array configuration, coupled with beam steering and advanced signal processing methods, heralds a promising future for the widespread adoption of such innovative sensors.

ACKNOWLEDGMENTS

The authors gratefully acknowledge the support of TUBITAK's Industry Innovation Network Mechanism (SAYEM) Program under grant no. 121D010 (Akıllı Ev Platformu) in collaboration with Eczacıbaşı. H.V.Demir also acknowledges support from TUBA and TUBITAK 2247-A National Leader Researchers Program (121C266). All authors thank to Mr. Fatih Gerenli and Eczacıbaşı team members for fruitful discussions on smart bathroom applications and further thank Eczacıbaşı for providing us with a sample of ceramic container.

REFERENCES

- [1] K. D. Frederick and D. C. Major, "Climate change and water resources," *Climate Change*, vol. 37, pp. 7-23, 1997.
- [2] N. W. Arnell, *Global warming, river flows and water resources*, Chichester: John Wiley & sons Ltd, 1996.
- [3] D. P. Lettenmaier, A. W. Wood, R. N. Palmer, E. F. Wood and E. Z. Stakhiv, "water resources implications of global warming: A U.S. regional perspective," *Climate Change*, vol. 43, pp. 537-579, 1999.
- [4] "www.epa.gov," 2 June 2014. [Online]. Available: <https://www.epa.gov/watersense/residential-toilets#tab-3>. [Accessed 18 Oct 2023].
- [5] W. H. Smolinski, "Water saver toilet bowl flush". United States of America Patent 3758893, 18 September 1973.
- [6] S. Lunt, "Low flush toilet system". United States of America Patent 9399863 B2, 26 July 2016.
- [7] M. Henini and M. Razeghi, "Handbook of Infra-red Detection Technologies," Elsevier, 2022.
- [8] Q. JINPING and L. XINGYUN, "Toilet flushing device for intelligently recognizing urine and excrement". China Patent CN201850614U, 26 June 2018.
- [9] A. Cataldo, G. Monti, E. D. Benedetto, G. Cannazza and L. Tarricone, "A Noninvasive Resonance-Based Method for Moisture Content Evaluation Through Microstrip Antennas," *IEEE Transactions of instrumentation and Measurement*, vol. 58, pp. 1420-1426, 2009.
- [10] K. Sarabandi and E. S. Li, "Microstrip Ring Resonator for Soil Moisture Measurements," *IEEE Transactions on Geoscience and Remote Sensing*, vol. 35, pp. 1223-1231, 1997.
- [11] M. Q.-L. R. f. D. C. o. L. Mixtures, "Larbi Benkhaoua; Mohamed Taoufik Benhabiles; Smail Mouissat; Mohamed Lahdi Riabi," *IEEE Sensors Journal*, vol. 16, pp. 1603-1610, 2016.
- [12] K.-C. Yoon, K.-G. Kim, J.-W. Chung and B.-S. Kim, "Low-Phase-Noise Oscillator Using a High-QL Resonator with Split-Ring Structure and Open-Loaded T-Type Stub for a Tumor-Location-Tracking Sensor," *Applied Sciences*, vol. 11, 2021.
- [13] A. M. Albishi, S. A. Alshebeili and O. M. Ramahi, "Three-Dimensional Split-Ring Resonators-Based Sensors for Fluid Detection," *IEEE Sensors Journal*, vol. 21, pp. 9138-9147, 2021.
- [14] L. Benkhaoua, S. Mouissat, M. T. Benhabiles, Y. Yakhlef and M. L. Riabi, "Miniaturized planar resonator for bio-sensing field," in *First IEEE MTT-S International Microwave Bio Conference*, Gothenburg, 2017.
- [15] E. C. Brdette, F. L. Cain and J. Seals, "In vivo prove measurement technique for determining dielectric properties at VHF through microware frequencies," *IEEE Transactions on Microwave Theory and Techniques*, vol. 28, 1980.
- [16] E. Yildiz and M. Bayrak, "A different Method Determining Dielectric Constant of Soil and Its FDTD simulation," *Mathematical & Computational Applications*, vol. 8, pp. 303-310, 2003.

- [17] A. Al-Fraihat, A. Al-Mufti, U. Hashim and T. Adam, "Potential of Urine Dielectric Properties in Classification of Stages of Breast Carcinomas," in *international conference on Electronic Design*, Penang, 2014.
- [18] M. Saadat-Safa, V. Nayyeri, A. Ghadimi, M. Soleimani and O. M. Ramahi, "A Pixelated Microwave Near-Field Sensor for Precise Characterization of Dielectric Materials," *Scientific reports*, 2019.
- [19] M. H. Zarifi and M. Daneshmand, "Wide dynamic range microwave planar coupled ring resonator for sensing applications," *Applied Physics Letters*, vol. 108, 2016.
- [20] M. H. Zarifi, T. Thundat and M. Daneshmand, "High resolution microwave microstrip resonator for sensing applications," *Sensors and Actuators*, 2015.
- [21] A. A. M. Bahar, Z. Zakaria, M. K. M. Arshad, A. A. M. Isa, Y. Darsil and R. A. Alahnomi, "Real Time Microwave Biochemical Sensor Based on Circular SIW Approach for Aqueous Dielectric Detection," *Scientific Reports*, 2019.
- [22] W. Withayachumnankul, K. Jaruwongrungrasamee, A. Tuantranont, C. Fumeaux and D. Abbott, "Metamaterial-based microfluidic sensor for dielectric characterization," *Sensors and Actuators*, 2012.
- [23] Z. Abbasi, M. Baghelani, M. Nosrati, A. Sanati-Nezhad and M. Daneshmand, "Real-Time Non-Contact Integrated Chipless RF Sensor for Disposable Microfluidic Applications," *IEEE Journal of Electromagnetics, RF and Microwave in Medicine and Biology*, vol. 4, 2020.
- [24] J. G. D. Oliveira, J. G. D. Junior, E. N. M. G. Pinto, V. P. S. Neto and A. G. D'Assunção, "A New Planar Microwave Sensor for Building Materials Complex Permittivity Characterization," *Sensors*, 2020.
- [25] A. Soffiatti, Y. Max, S. G. Silva and L. M. d. Mendonça, "Microwave Metamaterial-Based Sensor for Dielectric Characterization of Liquids," *Sensors*, 2018.
- [26] M. Ozturk, U. K. Sevim, O. Akgol, E. Unal and M. Karaaslan, "Determination of Physical Properties of Concrete by Using Microwave Nondestructive Techniques," *Aces Journal*, vol. 33, pp. 265-272, 2018.
- [27] M. T. Islam, M. N. Rahman, M. S. J. Singh and M. Samsuzzaman, "Detection of Salt and Sugar Contents in Water on the Basis of Dielectric Properties Using Microstrip Antenna-Based Sensor," *IEEE Access*, vol. 6, pp. 4118-4126, 2018.
- [28] M. H. Zarifi and M. Daneshmand, "Liquid sensing in aquatic environment using high quality planar microwave resonator," *Sensors and Actuators B*, pp. 517-521, 2015.
- [29] M. H. Zarifi and M. Daneshmand, "Monitoring Solid Particle Deposition in Lossy Medium Using Planar Resonator Sensor," *IEEE Sensors Journal*, vol. 17, pp. 7981-7989, 2-17.
- [30] M. H. Zarifi, M. Rahimi and M. Daneshmand, "Microwave ring resonator-based non-contact interface sensor for oil sands applications," *Sensors and Actuators B*, pp. 633-639, 2015.
- [31] N. Nguyen-Trong and C. Fumeaux, "Tuning Range and Efficiency Optimization of a Frequency-Reconfigurable Patch Antenna," *IEEE ANTENNAS AND WIRELESS PROPAGATION LETTERS*, vol. 17, pp. 150-154, 2018.
- [32] D. M. Pozar, in *Microwave Engineering*, John Wiley & Sons, Inc, 2012, pp. 228-271.
- [33] C. A. Balanis, in *Antenna theory analysis and design*, John Wiley and Sons, Inc, 2016, pp. 783-873.
- [34] F. Ghaderinezhad, H. C. Koydemir, D. Tseng, D. Karınca, K. Liang, A. Ozcan and S. Tasoglu, "Sensing of electrolytes in urine using a miniaturized paper-based device," *Scientific Reports*, vol. 10, 2020.
- [35] K. W. a. E. Litwiller, J. W. Fisher and J. Hogan, "Simulated Human Feces for Testing Human Waste Processing Technologies in Space Systems," in *36th International Conference on Environmental Systems (ICES)*, Norfolk, 2006.
- [36] K. Nörtemann, J. Hilland and U. Kaatz, "Dielectric Properties of Aqueous NaCl Solutions at Microwave Frequencies," *The Journal of Physical Chemistry A*, vol. 101, p. 6864-6869, 1997.
- [37] A. Stogryn, "Equations for Calculating the Dielectric Constant of Saline Water (Correspondence)," *IEEE Transactions on Microwave Theory and Techniques*, vol. 19, no. 8, pp. 733-736, 1971.
- [38] J. B. Hubbard, L. Onsager, W. M. V. Beek and M. Mandel, "Kinetic Polarization Deficiency in Electrolyte Solutions," *Proceedings of the National Academy of Sciences of the United States of America*, vol. 74, no. 2, pp. 401-404, 1977.
- [39] J. A. Lane and J. A. Saxton, "Dielectric Dispersion in Pure Polar Liquids at Very High Radio Frequencies. III. The Effect of Electrolytes in Solution," *Proceedings of the Royal Society of London. Series A, Mathematical and Physical Sciences*, vol. 214, no. 1119, pp. 531-545, 1952.
- [40] V. Kumar, J. V. Dhabalia, G. G. Nelivigi and M. S. Punia, "Age, gender, and voided volume dependency of peak urinary flow rate and uroflowmetry nomogram in the Indian population," *Indian Journal of Urology*, vol. 25, pp. 461-466, 2009.
- [41] R. Salmon, Introduction to Ocean Waves, San Diego: Scripps Institution of Oceanography, UC San Diego.



Sobhan Gholami joined the Bilkent University Department of Electrical and Electronics Engineering in 2021 as a research graduate student. Prior to his graduate studies, he was an undergraduate researcher at the bioMEMs laboratory of the Department of Electrical and Electronics Engineering at Marmara University, Istanbul-Turkey where he completed his undergraduate studies in 2021. He is currently pursuing his MSc. degree focusing on microwave sensors. His research interests are in electromagnetic theory and application, antenna/microwave theory and measurement.



Emre Unal received the B.Sc. degree in electrical and electronics engineering from Hacettepe University, Ankara, Turkey, in 2005. He is a full-time Research Engineer at the Institute of Materials Science and Nanotechnology, Bilkent University, Ankara, under the supervision of Prof. H. V. Demir, where he is working on the development of microwave and optoelectronic devices.



Hilmi Volkan Demir (M'04–FM'21) received the B.Sc. degree in electrical and electronics engineering from Bilkent University, Ankara, Turkey, in 1998, and the M.Sc. and Ph.D. degrees in electrical engineering from Stanford University, Stanford, CA, USA, in 2000 and 2004, respectively. In 2004, he joined Bilkent University, where he is currently a professor with joint appointments with the Department of Electrical and Electronics Engineering, Department of Physics and Institute of Materials Science and Nanotechnology (UNAM). He is also a Fellow of the National Research Foundation in Singapore and a Professor with Nanyang Technological University. His research interests include the development of innovative optoelectronic and RF devices. He is a member of Turkish Academy of Science.